Progress In Electromagnetics Research M, Vol. 102, 117–126, 2021

Feedforward Decoupling Control of Interior Permanent Magnet Synchronous Motor with Genetic Algorithm Parameter Identification

Yanfei Pan, Xin Liu*, Yilin Zhu, Bo Liu, and Zhongshu Li

Abstract—The goal of vector control of interior permanent magnet synchronous motor (IPMSM) is to make IPMSM have excellent dynamic and steady-state performance, but there is coupling between the *d*-*q* axis in the synchronous rotating coordinate system, which affects the torque response performance. In view of the fact that the traditional voltage compensation strategy is sensitive to the change of motor parameters, genetic algorithm is introduced to identify the parameters, and a feedforward voltage compensation control based on genetic algorithm parameter identification is proposed. The compensation voltage is calculated by the inductance and flux value of the motor identified by genetic algorithm. Compensation voltage is used to counteract the change of feedback voltage caused by the change of motor parameters in feedforward decoupling control. Simulated and experimental results show that the proposed strategy can effectively achieve *d*-*q* axis current decoupling, improve the dynamic performance of the system, and have excellent robustness.

1. INTRODUCTION

Permanent magnet synchronous motor (IPMSM) is widely used in the field of new energy vehicles because of its advantages of simple structure, reliable operation, high efficiency, high power factor, large starting torque, and good force and energy index [1, 2]. Vector control is a common control strategy in IPMSM. After coordinate transformation, static decoupling between *d*-axis subsystem and *q*-axis subsystem can be realized, but dynamic coupling is not eliminated. Therefore, when a control subsystem has a dynamic disturbance, it will inevitably affect another control subsystem and reduce the reliability of the system dynamic operation. Decoupling control technology is an effective way to solve the above problems. Through decoupling control, the coupling fluctuation between *d*-*q* axis control loops can be eliminated [3, 4].

Vector control realizes the decoupling between stator current excitation component and torque component. At present, the decoupling methods mainly include: voltage feedforward decoupling, current feedback decoupling, internal mode decoupling, deviation decoupling, etc. [5]. In [6], a nonlinear controller based on state feedback linearization is designed such that the nonlinear system with multivariable and strongly coupled motion is reduced to decoupled linear subsystems including its speed and rotor flux as well as two rotor displacements. But its robustness is decreased. In order to improve the robustness of the control system (the problem of robustness degradation caused by feedback linearization), the sliding mode control method is employed, and a novel double power reaching law is introduced to establish a feedback linearized sliding mode control system for PMSM drive system [7]. Although this method is robust against dynamic parameter changes, there will be oscillation in the process of system regulation. Aiming at the oscillation problem in the system, the strategy of using adaptive disturbance observer to observe the disturbance on the basis of internal mode is proposed [8, 9]. The strategy improves the steady-state performance of the system and has strong robustness, but the

Received 29 March 2021, Accepted 30 April 2021, Scheduled 30 April 2021
* Corresponding author: Xin Liu (xin.liu.dy@gmail.com).
The authors are with the Jiangsu Changjiang Intelligent Manufacturing Research Institute Co, Ltd, Changzhou 213001, China.

dynamic process is still overshoot. In addition, a feed-forward decoupling scheme is widely used because of short computing time and simple implementation [10].

However, feedforward decoupling can completely eliminate d-q axis coupling only if motor parameters are fixed. In fact, the motor parameters change with different operations of the motor, which will lead to incomplete decoupling and affect the system performance. In view of the above problems, the main solution is to identify the motor parameters online. With the development of computer technology and intelligent control technology, artificial intelligence algorithm with powerful nonlinear system processing ability and optimization ability has a wider application in the parameter identification of IPMSM. This kind of intelligent algorithm transforms IPMSM parameter identification problem into a system optimization problem. The algorithm mainly includes neural network algorithm [11, 12], particle swarm optimization algorithm (PSO) [13, 14], genetic algorithm (GA) [15, 16], etc. Among them, the neural network algorithm needs a large number of samples to train the algorithm, which will increase the time cost. The PSO algorithm is easy to fall into local optimum. Therefore, genetic algorithm is a powerful tool for solving nonlinear multi-parameter optimization problems because of its good global search ability and strong robustness.

Therefore, genetic algorithm is introduced to identify the IPMSM motor parameters online to improve the accuracy of system identification. The basic idea is to calculate the compensation voltage by the inductance and flux value of the motor identified by genetic algorithm, so as to counteract the change of the feedback voltage caused by the change of motor parameters in the feedforward decoupling control. Firstly, the IPMSM mathematical model is derived. After that, genetic algorithm and the principle of motor parameter identification of IPMSM are introduced. Based on this, a feedforward decoupling controller based on genetic algorithm parameter identification is constructed. Matlab/Simulink is used to compare the decoupling performance of the proposed control strategy and the traditional feedforward controller. Finally, the experimental platform is built for experimental verification.

2. IPMSM MODELING

In order to facilitate the analysis, the following assumptions can be adopted to simplify the mathematical model of the IPMSM by ignoring some less influential parameters:

1) Ignore the spatial harmonics; set the three-phase windings to be symmetrically placed in space; and the generated magnetomotive force is sinusoidally distributed along the circumference of the air gap.
2) Ignore core loss.
3) Ignore the damping winding of the rotor.

Therefore, in the d- and q-axis coordinate system, the mathematical model of IPMSM can be expressed as:

$$\begin{cases} u_d = L_d \dfrac{\mathrm{d}i_d}{\mathrm{d}t} - \omega_e L_q i_q + R i_d \\ u_q = L_q \dfrac{\mathrm{d}i_q}{\mathrm{d}t} + \omega_e L_d i_d + \omega_e \psi_f + R i_q \end{cases} \tag{1}$$

where u_d and u_q are the stator voltages of d-axis and q-axis, respectively; i_d and i_q are the stator currents of d-axis and q-axis, respectively; L_d and L_q are stator inductances of d-axis and q-axis, respectively; R is the stator resistance; ω_e is the electrical angular velocity; ψ_f is the rotor flux.

3. PRINCIPLE OF PARAMETER IDENTIFICATION OF IPMSM

Suppose that the dynamic mathematical model of the identified system is as follows:

$$\begin{cases} \dot{\mathbf{x}} = f(\boldsymbol{\theta}, \mathbf{x}, \mathbf{u}) \\ \mathbf{y} = \mathbf{C}\mathbf{x} \end{cases} \tag{2}$$

where $\mathbf{x}$ is the state variable, $\boldsymbol{\theta}$ the parameter to be identified, $\mathbf{u}$ the input variable, and $\mathbf{C}$ a constant matrix.

The tracking system of the above system is expressed as:

$$\begin{cases} \hat{\dot{\mathbf{x}}} = f(\hat{\boldsymbol{\theta}}, \hat{\mathbf{x}}, \mathbf{u}) \\ \hat{\mathbf{y}} = C\hat{\mathbf{x}} \end{cases} \tag{3}$$

where $\hat{\mathbf{x}}$ is the state variable of the tracking system, $\hat{\boldsymbol{\theta}}$ the estimated value of $\boldsymbol{\theta}$, and $\hat{\mathbf{y}}$ the estimated value of $\mathbf{y}$.

Convert the form of Equation (1) into the form of current equation:

$$\begin{cases} \dfrac{\mathrm{d}i_d}{\mathrm{d}t} = \frac{u_d}{L_d} - \dfrac{L_q}{L_d}\omega_e i_q - \frac{Ri_d}{L_d} \\ \dfrac{\mathrm{d}i_q}{\mathrm{d}t} = \dfrac{u_q - \omega_e\psi_f}{L_q} - \dfrac{Ri_q}{L_q} - \frac{\omega_e L_d i_d}{L_q} \end{cases} \tag{4}$$

Since the actual control system is a discrete control system, the current equation needs to be discretized. Rewrite the d- and q-axis current equations in Equation (4) by using the Pade approximation method and discretizing it:

$$\begin{cases} i_d(k) = \theta_{d1} i_d(k-1) + \theta_{d2}[\omega_e(k) i_q(k) + \omega_e(k-1) i_q(k-1)] + \theta_{d3}[u_d(k) + u_d(k-1)] \\ i_q(k) = \theta_{q1} i_q(k-1) + \theta_{q2}[\omega_e(k) i_d(k) + \omega_e(k-1) i_d(k-1)] + \theta_{q3}[u_q(k) + u_q(k-1)] \\ \qquad +\theta_{q4}[\omega_e(k) + \omega_e(k-1)] \end{cases} \tag{5}$$

The parameters in the equation are:

$$\begin{cases} \theta_{d1} = \dfrac{-T_s R + 2L_d}{T_s R + 2L_d} \\ \theta_{d2} = \dfrac{L_q T_s}{T_s R + 2L_d} \\ \theta_{d3} = \dfrac{T_s}{T_s R + 2L_d} \\ \theta_{q1} = \dfrac{-T_s R + 2L_q}{T_s R + 2L_q} \\ \theta_{q2} = \dfrac{-L_d T_s}{T_s R + 2L_q} \\ \theta_{q3} = \dfrac{T_s}{T_s R + 2L_q} \\ \theta_{q4} = \dfrac{-T_s \psi_f}{T_s R + 2L_q} \end{cases} \Rightarrow \begin{cases} R = \dfrac{1 - \theta_{q1}}{2\theta_{q3}} = \dfrac{1 - \theta_{d1}}{2\theta_{d3}} \\ L_d = -\dfrac{\theta_{q2}}{\theta_{q3}} = \dfrac{1 + \theta_{d1}}{4\theta_{d3}} T_s \\ L_q = \dfrac{1 + \theta_{q1}}{4\theta_{q3}} T_s = \dfrac{\theta_{d3}}{\theta_{d3}} \\ \psi_f = -\dfrac{\theta_{q4}}{\theta_{q3}} \end{cases} \tag{6}$$

where T_s is the time interval between two discrete points.

Establish an equivalent tracking function as follows:

$$\begin{cases} \hat{i}_d(k) = \hat{\theta}_{d1} i_d(k-1) + \hat{\theta}_{d2}[\omega_e(k) i_q(k) + \omega_e(k-1) i_q(k-1)] + \hat{\theta}_{d3}[u_d(k) + u_d(k-1)] \\ \hat{i}_q(k) = \hat{\theta}_{q1} i_q(k-1) + \hat{\theta}_{q2}[\omega_e(k) i_d(k) + \omega_e(k-1) i_d(k-1)] + \hat{\theta}_{q3}[u_q(k) + u_q(k-1)] \\ \qquad +\hat{\theta}_{q4}[\omega_e(k) + \omega_e(k-1)] \end{cases} \tag{7}$$

When the deviation between the predicted current and actual current is less than a certain accuracy, it can be considered that the estimated parameters at this time are close to the actual parameters. The identification of motor parameters R, L_d, L_q, and ψ_f can be equivalent to the identification of parameters θ_{d1}, θ_{d2}, θ_{d3}, θ_{q1}, θ_{q2}, θ_{q3}, and θ_{q4}, and the motor parameters can be deduced by Equation (6).

4. APPLICATION OF GENETIC ALGORITHM IN MOTOR PARAMETER IDENTIFICATION

Genetic algorithm has the advantages of fast search speed, simple algorithm, wide range of adaptability, and good convergence. Therefore, genetic algorithm is used to identify the parameters of IPMSM in this paper.

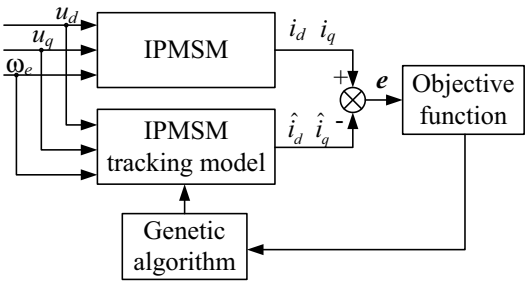

Figure 1. Block diagram of genetic algorithm parameter identification.

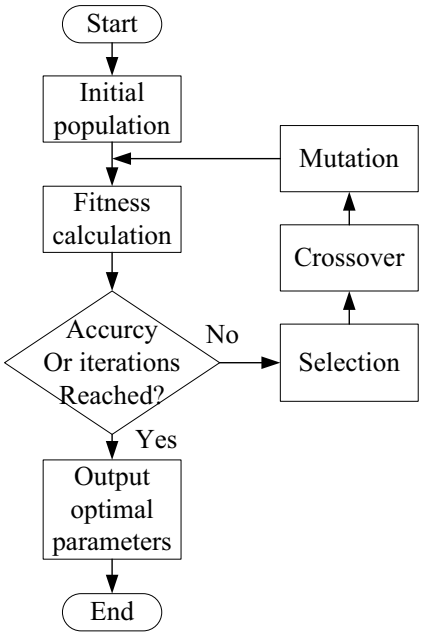

Figure 2. Genetic algorithm flow chart.

Figure 1 shows the block diagram of genetic algorithm parameter identification. First, calculate the initial parameters of the motor according to the nameplate of the motor, and estimate the range of the motor parameters based on engineering experience. From this, determine the number of bits and search accuracy of the binary code in the genetic algorithm. The genetic algorithm flowchart is shown in Figure 2. Randomly generate the initial population. The population size is 20, and each chromosome is composed of 4 motor parameters through binary coding. When the initial parameters of the GA output are input into the IPMSM tracking model, the current deviation is input into the GA objective function. The objective function equation is as follows:

$$J(\theta) = \sum_{k=0}^{n-1} \left\{ \left[i_d(k) - \hat{i}_d(k) \right]^2 + \left[i_q(k) - \hat{i}_q(k) \right]^2 \right\} \tag{8}$$

where n is the number of discrete points collected in a sampling period.

According to the objective function, the fitness of each individual is calculated, and the selection, crossover, and mutation operation are performed to obtain the next generation population. Repeat the above operations until the objective function reaches the set accuracy or reaches the preset number of iterations of genetic algorithm.

Figure 3 is the block diagram of genetic algorithm parameter identification feedforward decoupling control. Use the estimated value of the IPMSM parameters identified by the genetic algorithm to

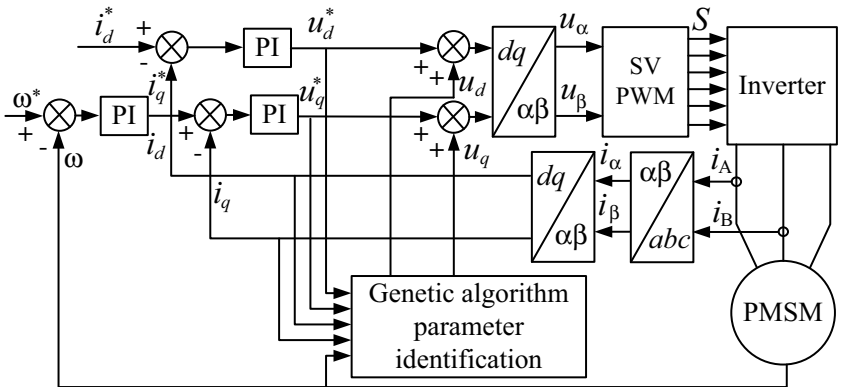

Figure 3. Genetic algorithm parameter identification feedforward decoupling control block diagram.

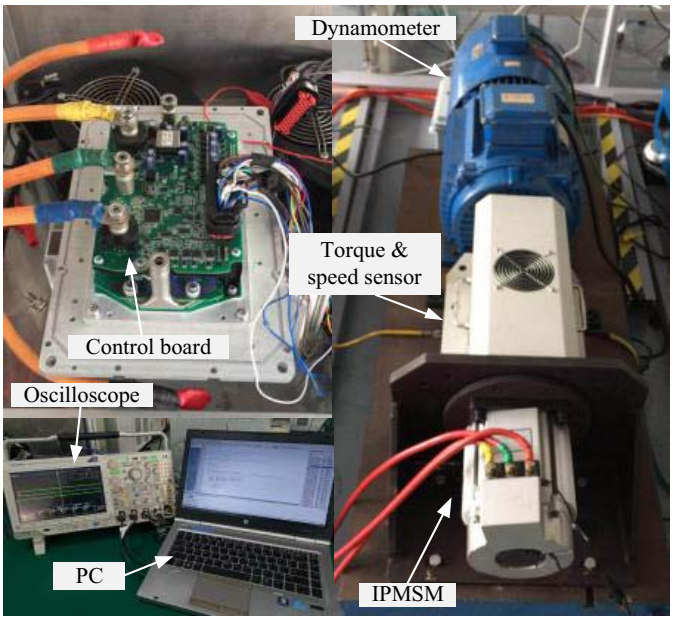

Figure 4. Experimental platform.

calculate the compensation voltage u_d, u_q, and feed forward into the forward channel of the control block diagram to realize the online parameter identification and feedforward decoupling of the IPMSM.

5. SIMULATION AND EXPERIMENTAL RESULTS

In this experiment, an experimental platform for the IPMSM vector control system is set up. The input of the genetic algorithm module is the stator voltage, stator current, and motor speed of the motor. Table 1 shows the motor parameters.

The parameter identification algorithm requires the stator voltage, stator current, and the first derivative of each sampling point. The interference of noise has a great influence on the calculation result, so a second-order Butterworth low-pass filter is used to filter the sampled voltage and sampled current, and the cut-off frequencies are 10 Hz and 5 Hz, respectively. Figure 4 shows the experimental platform.

Table 1. Parameter of the motor.

Symbol	Value	Symbol	Value
P_n/W	20	n/(r/min)	3600
U_{dc}/V	96	R/Ω	0.006
I_n/A	190	L_d/μH	68.3
ψ_f/Wb	0.03	L_q/μH	189.0
T_e/(N·m)	54	P	4

5.1. Genetic Algorithm Parameter Identification and Fitting Accuracy

The genetic algorithm is used for parameter identification, and the binary coding method is adopted. The coding length of each parameter is 10 bits. According to the motor parameters in Table 1, set the parameter selection ranges of R, L_d, L_q, and ψ_f to 0–0.01 Ω, 50–100 μH, 150–200 μH, 0–0.05 Wb. Express the accuracy of the four parameters (R, L_d, L_q, and ψ_f) as e_1, e_2, e_3, and e_4:

$$\begin{cases} e_1 = \dfrac{0.01}{2^{10}-1} = 9.7752 \times 10^{-6}\,\Omega \\ e_2 = \dfrac{50}{2^{10}-1} = 0.0489\,\mu\text{H} \\ e_3 = \dfrac{50}{2^{10}-1} = 0.0489\,\mu\text{H} \\ e_4 = \dfrac{0.05}{2^{10}-1} = 4.8876 \times 10^{-5}\,\text{Wb} \end{cases} \tag{9}$$

The crossover rate is set to 0.6; the mutation rate is set to 0.01; the population size is 20; the number of iterations is set to 500; and the system control cycle is 0.1 ms.

When the motor is running at zero d-axis current; the load torque is half of the motor rated torque; and the motor speed is 3600 r/min, as shown in Figure 5, it is the objective function curve during 500 generations of genetic algorithm iteration. It can be found that genetic algorithm has the advantages

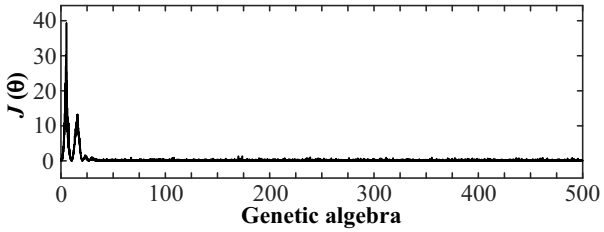

Figure 5. Objective function curve.

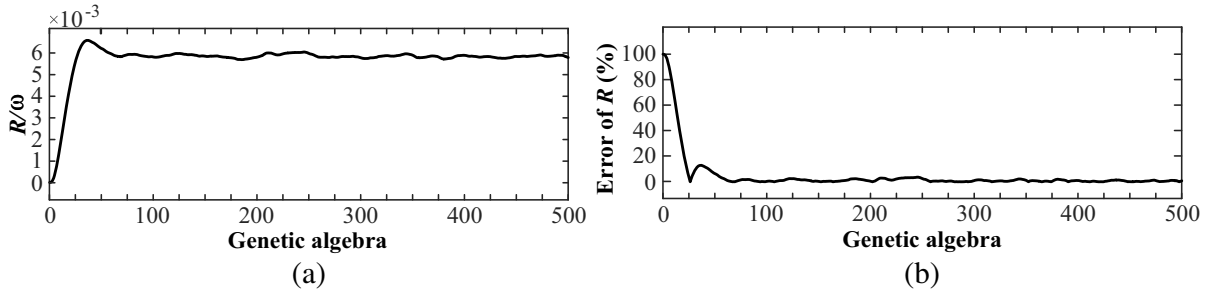

Figure 6. Identification value and accuracy of R.

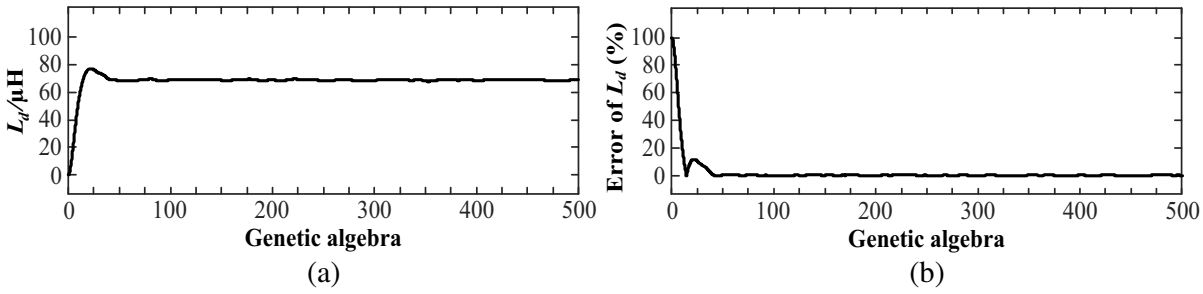

Figure 7. Identification value and accuracy of L_d.

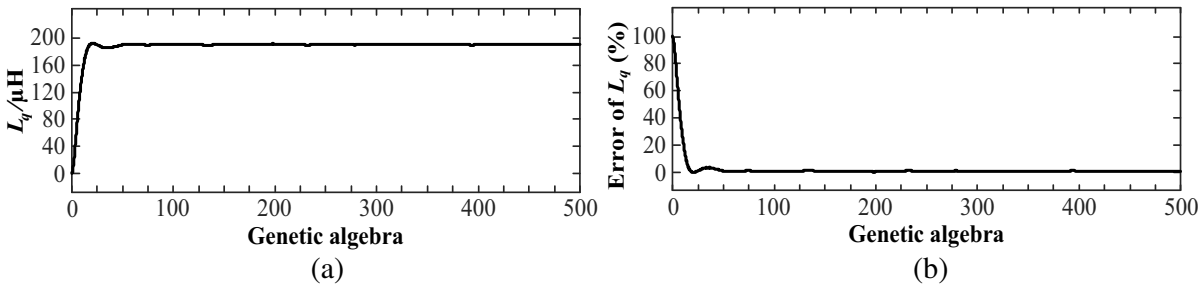

Figure 8. Identification value and accuracy of L_q.

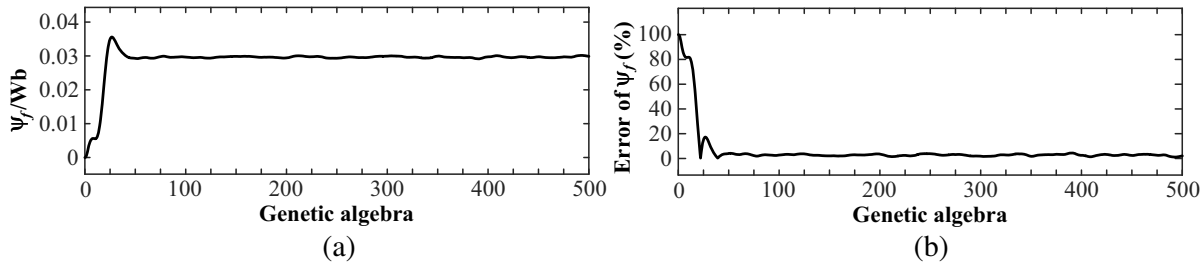

Figure 9. Identification value and accuracy of ψ_f.

of fast convergence speed and high accuracy, and it has converged to a relatively high level of accuracy around 50 generations.

The genetic algorithm identification experiment results are shown in Figures 6–9. As can be seen from the above figure, the four parameters can converge to the true value very well, and the accuracy can be controlled at about 3%, indicating that the genetic algorithm has a good identification effect.

5.2. Decoupling Control Based on Genetic Algorithm Parameter Identification

The voltage feedforward decoupling control strategy is simple in structure, easy to implement, and widely used in industrial process control. By designing a voltage compensator to offset the coupling voltage generated by the d- and q-axis current coupling, the dynamic control performance of the system is greatly improved. However, the traditional voltage feedforward decoupling largely depends on the motor parameters. When the motor parameters change, the coupling effect becomes more serious, and the decoupling cannot be fully realized. Using the genetic algorithm parameter identification strategy, the real-time identification of the motor parameters is input to the voltage compensation module, which can solve the problem that the compensated feedforward voltage does not match the motor model due to the change of the motor parameters.

The feedforward compensation voltage in Figure 3 can be expressed as:

$$\begin{cases} u_d = -\omega_e \hat{L}_q i_q \\ u_q = \omega_e \hat{L}_d i_d + \omega_e \hat{\psi}_f \end{cases} \tag{10}$$

where $\hat{L}_d$, $\hat{L}_q$, and $\hat{\psi}_f$ are the estimated values of L_d, L_q, and ψ_f, respectively.

Due to the fast iteration speed of the genetic algorithm, it can complete the iteration of the current sampling value within a 0.1 ms control period, so the identified parameter values are updated online in the voltage compensation module in real time to achieve real-time voltage feedforward online decoupling.

Figure 10 shows the coupling relationship of d- and q-axis currents in IPMSM without feedforward voltage compensation, traditional feedforward voltage compensation, and feedforward voltage compensation with parameter identification.

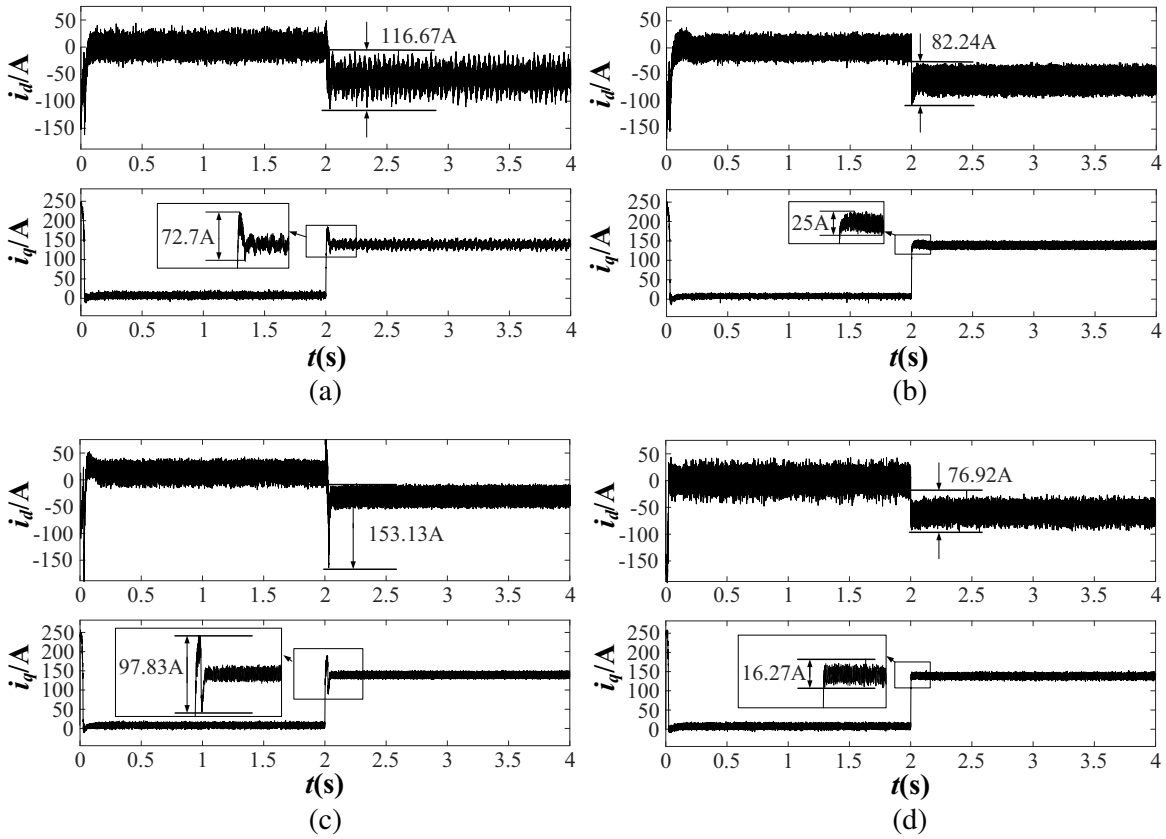

Figure 10. Decoupling performance of d- and q-axis currents. (a) No feedforward decoupling. (b) Traditional feedforward decoupling. (c) Neural network feedforward decoupling. (d) Feedforward decoupling method proposed in this paper.

In the first two seconds, the motor was running at no-load state, and then half of the rated load was suddenly added. It can be observed that without feedforward compensation, as shown in Figure 10(a), the d- and q-axis currents fluctuate greatly when the load is suddenly applied, and the overshoot is respectively 116.67 A and 72.7 A. This is caused by the coupling existing in the d- and q-axis currents. Traditional feedforward compensation, as shown in Figure 10(b), compared with no feedforward compensation, the d- and q-axis currents have a certain improvement, but there is still a certain fluctuation when the load changes, and the overshoot is 82.64 A, 25 A, because the compensation voltage does not match the actual parameters of the motor. Neural network feedforward compensation, as shown in Figure 10(c), has good steady-state performance, but when the load changes, the dq axis current overshoot is large, and the overshoot is respectively 153.13 A and 97.83 A. Figure 10(d) is the

method proposed in this article. When the load changes, there is no obvious fluctuation in the d- and q-axis currents, and the overshoot is only 76.92 A and 16.27 A, respectively. It shows that the decoupling effect of this method is good.

6. CONCLUSION

A decoupling control strategy based on genetic algorithm parameter identification is proposed to improve the accuracy of IPMSM decoupling control. With the change of motor operating condition, the IPMSM motor parameters will change obviously, and the coupling voltage of d-q axis cannot be calculated accurately. In this paper, the inductance and flux linkage of the motor are identified online by genetic algorithm, and the compensation voltage is calculated by using the identification results. The voltage change caused by the change of parameters is compensated. At the same time, the validity of the proposed control strategy is verified by building the simulation model and the experimental control system of IPMSM. The results show that the proposed method has good robustness and improves the performance of decoupling control.

REFERENCES

1. Han, Z.-X. and J.-L. Liu, "Comparative analysis of vibration and noise in IPMSM considering the effect of MTPA control algorithms for electric vehicles," *IEEE Transactions on Power Electronics*, Vol. 36, No. 6, 6850–6862, 2021.
2. Murakami, M., S. Morimoto, Y. Inoue, et al., "Maximum torque per ampere control of an IPMSM with magnetic saturation using online parameter identification," *Proceedings of 2020 23rd International Conference on Electrical Machines and Systems*, 1631–1636, Hamamatsu, Japan, 2020.
3. Fang, J.-C., Y.-Z. He, and Z.-Y. Wang, "Decoupling control strategy for high speed permanent magnet synchronous motor based on inversion system method," *2014 IEEE Workshop on Advanced Research and Technology in Industry Applications*, 895–898, Ottawa, Canada, 2014.
4. Guo, J., T. Fan, Q. Li, e al., "Coupling and digital control delays affected stability analysis of permanent magnet synchronous motor current loop control," *Vehicle Power and Propulsion Conference*, 1–5, 2019.
5. Ban, F., G. Gu, and G. Lian, "Research on decoupling model predictive torque control strategy with load feedforward compensation for PMSM," *2020 IEEE International Conference on Applied Superconductivity and Electromagnetic Devicesbuzai*, 1–2, Tianjin, China, 2020.
6. Xiong, T., G. Zhou, and D.-D. Zou, "State feedback decoupling control of web tension velocity and lateral displacement in unwinding system," *Chinese Control and Decision Conference*, 5217–5224, 2020.
7. Chen, S.-Z., J.-F. Jiang, X.-H. Hou, et al., "Feedback linearized sliding mode control of PMSM based on a novel reaching law," *Electrical Machines and Systems International Conference*, 1438–1441, 2020.
8. Thieli, S. G., H. A. Grundling, and R. P. Vieira, "Sliding mode current control based on disturbance observer applied to permanent magnet synchronous motor," *Proceedings of 1st Southern Power Electronics Conference*, 1–6, Fortaleza, Brazil, 2015.
9. Scalcon, F. P., T. S. Gabbi, R. P. Vieira, et al., "Decoupled vector control based on disturbance observer applied to the synchronous reluctance motor," *Proceedings of 21st European Conference on Power Electronics and Applications*, P.1–P.8, Genova, Italy, 2019.
10. Gan, X.-Y., C. Liu, Y. Zuo, et al., "Analysis and dynamic decoupling control schemes for PMSM current loop," *IEEE International Conference on Aircraft Utility Systems*, 570–574, Beijing, China, 2016.
11. Lee, K. and J. Ha, "Dynamic decoupling control method for PMSM drive with cross-coupling inductances," *IEEE Applied Power Electronics Conference and Exposition*, 563–569, Tampa, FL, USA, 2017.

12. Jie, H., G. Zheng, J. Zou, et al., "Adaptive decoupling control using radial basis function neural network for permanent magnet synchronous motor considering uncertain and time-varying parameters," *IEEE Access*, Vol. 8, 112323–112332, 2020.
13. Calvini, M., M. Carpita, A. Formentini, et al., "PSO-based self-commissioning of electrical motor drives," *IEEE Transactions on Industrial Electronics*, Vol. 62, No. 2, 768–776, 2015.
14. Liu, Z., H.-L. Wei, Q.-C. Zhong, et al., "Parameter estimation for VSI-Fed PMSM based on a dynamic PSO with learning strategies," *IEEE Transactions on Power Electronics*, Vol. 32, No. 4, 3154–3165, 2017.
15. Avdeev, A. and O. Osipov, "PMSM identification using genetic algorithm," *International Workshop on Electric Drives: Improvement in Efficiency of Electric Drives*, 1–4, Moscow, Russia, 2019.
16. Song, Z., Y. Lin, X. Mei, et al., "A novel inertia identification method for servo system using genetic algorithm," *International Conference on Smart Grid and Electrical Automation*, 22–25, Zhangjiajie, China, 2016.